GFZ
Helmholtz-Zentrum
POTSDAM

Originally published as:

Lühr, H., Kervalishvili, G., Michaelis, I., Rauberg, J., Ritter, P., Park, J., Merayo, J. M. G., Brauer, P. (2015): The interhemispheric and F region dynamo currents revisited with the Swarm constellation. - *Geophysical Research Letters*, *42*, 9, p. 3069-3075.

DOI: http://doi.org/10.1002/2015GL063662

AGU PUBLICATIONS

Geophysical Research Letters

RESEARCH LETTER

10.1002/2015GL063662

Special Section:
ESA's Swarm Mission, One Year in Space

Key Points:
- Application of new approach for current determination is performed
- Characteristics of interhemispheric field-aligned currents is presented
- Characteristics of *F* region dynamo currents is presented

Correspondence to:
H. Lühr,
hluehr@gfz-potsdam.de

Citation:
Lühr, H., G. Kervalishvili, I. Michaelis, J. Rauberg, P. Ritter, J. Park, J. M. G. Merayo, and P. Brauer (2015), The interhemispheric and *F* region dynamo currents revisited with the Swarm constellation, *Geophys. Res. Lett.*, *42*, 3069–3075, doi:10.1002/2015GL063662.

Received 4 MAR 2015
Accepted 23 MAR 2015
Accepted article online 26 MAR 2015
Published online 4 MAY 2015

The interhemispheric and *F* region dynamo currents revisited with the Swarm constellation

Hermann Lühr[1], Guram Kervalishvili[1], Ingo Michaelis[1], Jan Rauberg[1], Patricia Ritter[1], Jaeheung Park[2], Jose M. G. Merayo[3], and Peter Brauer[3]

[1]German Research Centre for Geosciences, Potsdam, Germany, [2]Korea Astronomy and Space Science Institute, Daejeon, South Korea, [3]DTU Space, Technical University of Denmark, Lyngby, Denmark

Abstract Based on magnetic field data sampled by the Swarm satellite constellation it is possible for the first time to determine uniquely *F* region currents at low latitudes. Initial results are presented from the first 200 days of formation flight (17 April to 5 November 2014). Detailed results have been obtained for interhemispheric field-aligned currents connecting the solar quiet day magnetic variation (*Sq*) current systems in the two hemispheres. We obtain prominent currents from the Southern (winter) Hemisphere to the Northern around noon. Weaker currents in opposite direction are observed during morning and evening hours. Furthermore, we could confirm the existence of vertical currents above the dip equator, downward around noon and upward around sunset. For both current systems we present and discuss longitudinal variations.

1. Introduction

During times of low magnetic activity there exist current vortices in the ionospheric *E* region on the dayside, which is termed the solar quiet (*Sq*) current system [e.g., *Campbell*, 1989]. In the Northern Hemisphere the currents flow counterclockwise and in the Southern clockwise around the focus at 30°–35° magnetic latitude (MLAT) [e.g., *Matsushita and Maeda*, 1965; *Yamazaki et al.*, 2011]. The intensity of currents depends to first order on the solar extreme ultraviolet (EUV) radiation and the solar elevation angle (different between summer and winter hemisphere). The asymmetry in current strength during solstice seasons leads to a potential difference between the hemispheres [e.g., *van Sabben*, 1964] and is driving interhemispheric field-aligned currents (IHFACs) [*Fukushima*, 1979]. First observational evidence for IHFACs was provided by *Olsen* [1997], based on Magsat data and later by *Yamashita and Iyemori* [2002] from Ørsted and ground-based data. *Park et al.* [2011] made use of 9 years of CHAMP magnetic field measurements for deriving a climatology of IHFACs. In principle they could confirm the theoretical prediction that IHFACs flow from the winter to the summer hemisphere around noon and in the opposite direction during morning hours. Different from the prediction, *Park et al.* [2011] found summer to winter IHFACs also in the evening. This notion was particularly clear during the months May to September and outside the South Atlantic Anomaly. During November to March the effect of nonmigrating tides was somewhat modifying the IHFACs signature.

Similarly, the characteristics of the *F* region dynamo currents were also deduced from the 10 year CHAMP data set [*Park et al.,* 2010a]. The concept of a wind-driven *F* region dynamo above the dip equator was introduced by *Rishbeth* [1971]. Initial observational evidence for the existence of that current system came from Magsat [e.g., *Maeda et al.*, 1982] and from CHAMP [*Lühr and Maus*, 2006]. They showed that there is an upward flowing current above the dip equator around 18:00 local time (LT) and a downward current around noon. More details of the *F* region dynamo, including its dependence on season, longitude, and solar activity, were presented by *Park et al.* [2010a, 2010b].

A caveat of all these comprehensive studies is that they have been deduced from single-satellite magnetic field data. This required to make a number of assumptions. In practice, any deflection of the magnetic east-west component from the main field direction was attributed to either the IHFAC or the *F* region dynamo, depending whether it varies symmetrically or antisymmetrically about the dip equator. Any other field source had to be ignored. Different from that we can determine uniquely radial currents and field-aligned currents (FACs) from the Swarm pair Swarm-A and Swarm-C, which is flying side by side. It is the first time that these low-latitude *F* region currents are sampled without the need for assumptions.

©2015. American Geophysical Union. All Rights Reserved.

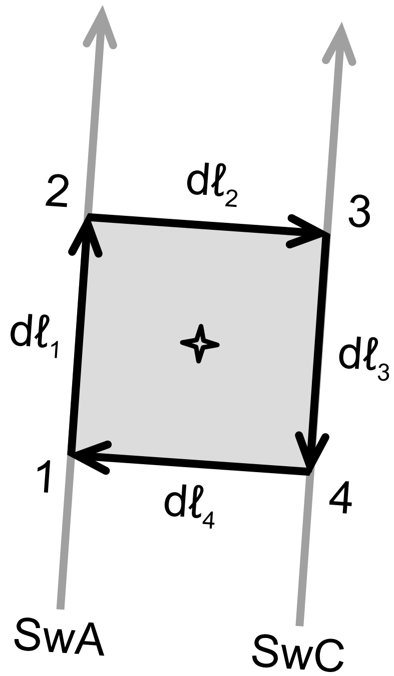

Figure 1. Sketch of the four measurement points and the integration passes for calculating the average current density flowing through the encircled area.

In the section to follow, we will first introduce the data and the processing approach. Subsequent sections are devoted to the observation of IHFACs and *F* region dynamo currents. In the discussion section we will compare our findings with earlier results and try to interpret the observed features.

2. Data and Processing Approach

European Space Agency (ESA)'s Earth observation mission Swarm was launched on 22 November 2013 into a near-polar orbit. The final constellation of the three-satellite mission was achieved on 17 April 2014. Since then the two satellites Swarm-A and Swarm-C fly side by side at an altitude of about 470 km. Swarm-B is cruising somewhat higher at 520 km. The satellites are equipped with a set of six instruments [see *Friis-Christensen et al.*, 2008]. Here we make use of the magnetic field vector data, sampled by the Vector Field Magnetometer (VFM). The vector data are calibrated against the Absolute Scalar Magnetometer (ASM), a Helium vapor instrument. This procedure ensures high accuracy of the independent data sets from the two spacecraft.

The vertical current density estimates are derived by applying Ampère's ring integral:

$$j = \frac{1}{\mu_0 A} \oint B \, \mathrm{d}l$$

where *A* is the area encircled by the contour, *B* the magnetic field caused by the current, d*l* the line element along the integration *path*, and μ_0 the permeability of free space. In practice we use four readings forming the corners of a quadrangle. As illustrated in Figure 1, there are two readings taken along the track, separated by 5 s, of both satellites. When considering the orbital velocity of 7.6 km/s this corresponds to a distance of 38 km. The cross-track separation between the two satellites amounts to 1.4° in longitude. For calculating the average vertical current density, j_z, within the encircled area we use a discrete form

$$j_z = \frac{1}{2\mu_0 A}\left[\left(B_{x_{t1}} + B_{x_{t2}}\right)\mathrm{d}l_1 + \left(B_{y_{t2}} + B_{y_{t3}}\right)\mathrm{d}l_2 - \left(B_{x_{t3}} + B_{x_{t4}}\right)\mathrm{d}l_3 - \left(B_{y_{t4}} + B_{y_{t1}}\right)\mathrm{d}l_4\right]$$

where B_x and B_y are the horizontal components aligned with the track and with the lines connecting the satellites, respectively; d*l* are the line elements between the corners, and $A = {}^1/_4(\mathrm{d}l_1 + \mathrm{d}l_2)(\mathrm{d}l_3 + \mathrm{d}l_4)$.

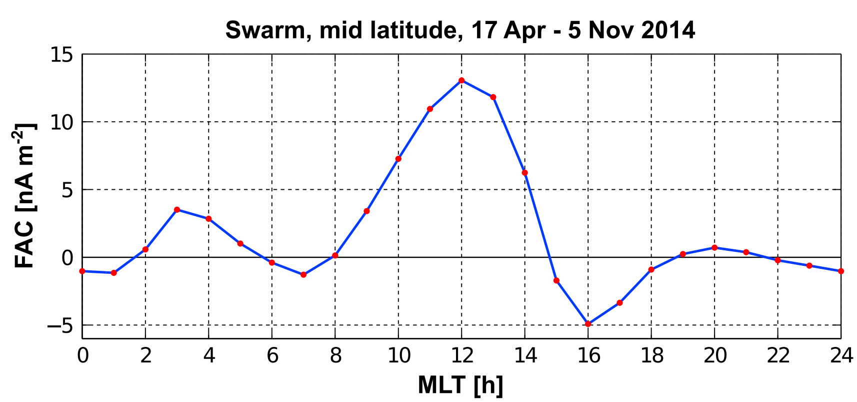

Figure 2. Local time dependence of the interhemispheric field-aligned current, average over the study period. Positive values represent currents flowing northward.

©2015. American Geophysical Union. All Rights Reserved.

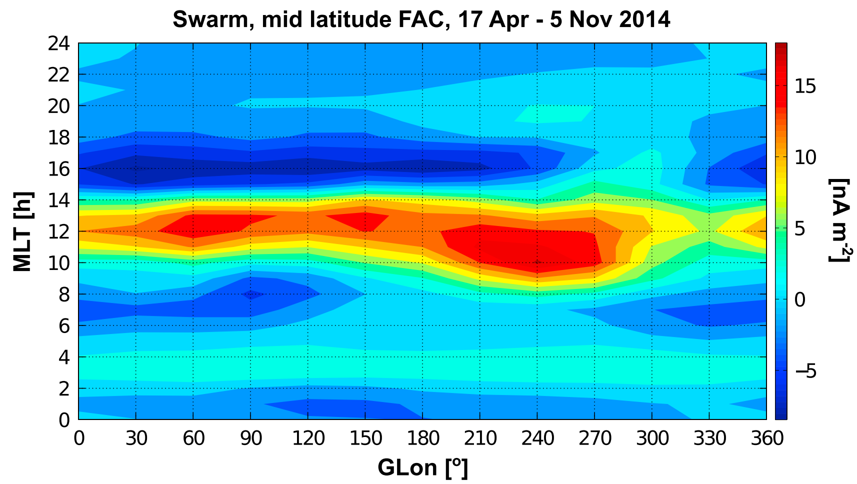

Figure 3. Local time versus longitude distribution of interhemispheric field-aligned currents. Positive values represent currents flowing northward.

In order to obtain the magnetic effect caused by the currents, the core field, crustal field, and large-scale magnetospheric field has to be subtracted from the original readings. Furthermore, the field residuals are low-pass filtered with a 3 dB cutoff period of 20 s, to avoid the effect of spatial aliasing. For estimating field-aligned currents (FACs) from the vertical current readings we have to consider the magnetic inclination, *I*

$$j_{||} = \frac{j_z}{\sin I}$$

We make use of this relation only for inclinations larger than 30°, not in the vicinity of the dip equator, in order to avoid too small numbers in the denominator. Further details of FAC calculation are given by *Ritter et al.* [2013].

3. The Interhemispheric Field-Aligned Currents

For the characterization of the IHFACs we made use of the dual-satellite FAC estimates as outlined in the previous section. The data interval used lasts from 17 April to 5 November 2014. It thus covers the June solstice and September equinox seasons. For quantifying the IHFAC intensity we calculated the average FAC density flowing in or out of the *E* region over the range of 20°–40° MLAT from the two hemispheres. This range safely includes the *Sq* focus latitude. In this way we obtain a single IHFAC value from each satellite passage over the equator.

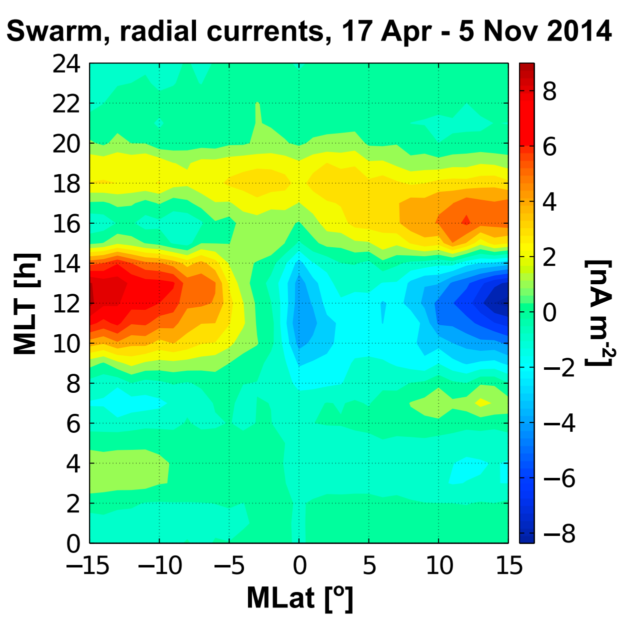

Figure 4. Local time versus magnetic latitude distribution of vertical *F* region currents. Positive values represent upward flowing currents.

Figure 2 shows the IHFAC variation with local time. Most prominent is the positive peak around noon reaching current densities of 13 nA/m^2. Positive values represent currents flowing from the Southern to the Northern Hemisphere. Opposite currents, however much weaker, are observed during the morning and evening hours. Such a current configuration is largely consistent with the prediction of *Fukushima* [1994, Figure 17] for June solstice conditions, except for the

©2015. American Geophysical Union. All Rights Reserved.

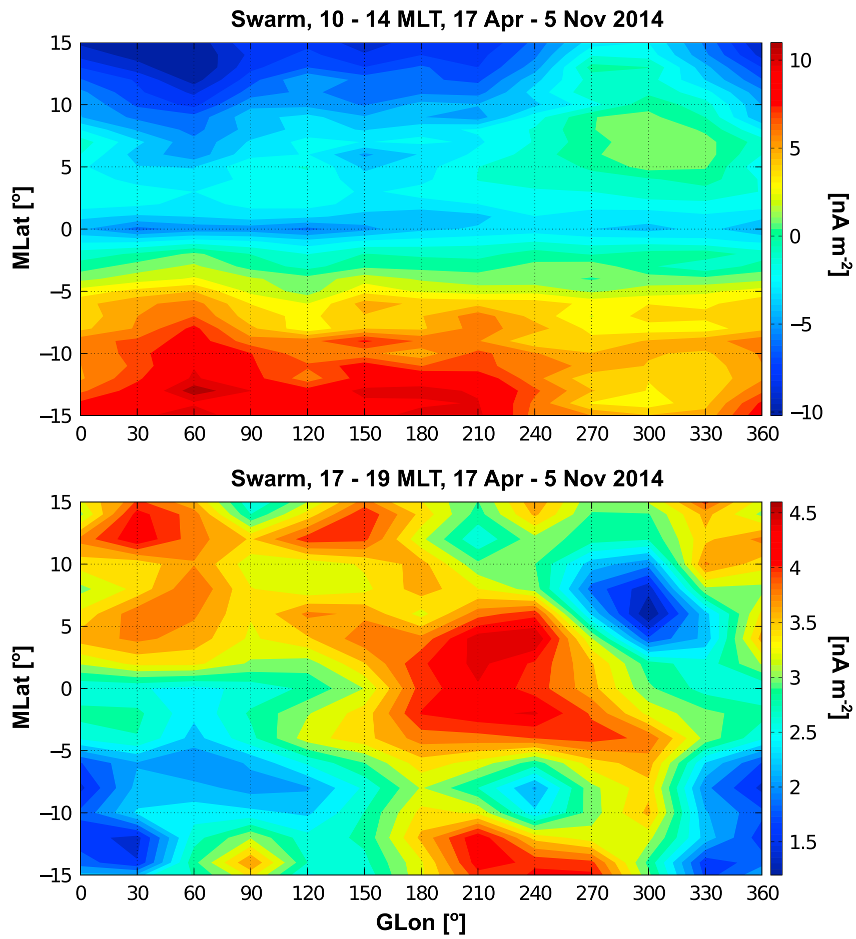

Figure 5. Magnetic latitude versus longitude distribution of vertical *F* region current (top) from noon sector and (bottom) from evening sector. Positive values represent upward flowing currents.

current direction in the evening sector. Somewhat unexpected is the northbound IHFAC around 03 magnetic local time (MLT). It does not seem to be related to the *Sq* system, and its interpretation is therefore considered to be beyond the scope of this study.

In Figure 3 we show how the IHFACs vary over longitude. Data have been sorted into 24 overlapping 2 h local time bins and into 12 overlapping 60° longitude bins. Clearly outstanding is again the positive current around noon. Also, the negative currents during morning and evening hours are well visible. Quite remarkable is the fading of the noontime IHFAC in the longitude range 300°E–350°E. Obviously, the potential difference between the hemispheres is reduced in this sector. Also worth noting, IHFACs peak at local times before noon in the sector 200°E–300°E geographic longitude (GLon). The weak northward current around 03 MLT shows no longitude variations.

4. Radial Currents Over the Dip Equator

In the vicinity of the equator no field-aligned currents have been estimated due to the small inclination. Figure 4 shows therefore the evolution of the radial current component over the day within the latitude range ±15° MLAT. Positive values represent upward currents. At latitudes higher than ±7° MLAT we recognize the features of the IHFACs appearing with opposite signs in the two hemispheres. There are the intense IHFACs around noon, the reverse currents around 07 and 16 MLT, and the weak postmidnight FACs.

Of particular interest for this section are the radial currents in close vicinity to the dip equator, which are attributed to the action of the *F* region dynamo. As expected, we find downward currents with peak densities

©2015. American Geophysical Union. All Rights Reserved.

of 3 nA/m^2 around noon and upward currents of comparable strength around 18 MLT. The polarity change around 15 MLT can be attributed to the switch of the zonal wind from westward to eastward at that time [e.g., *Liu et al.,* 2006]. The latitudinal width of the dynamo current is quite narrow, amounting to about ±2.5° around noon and ±5° at 18 MLT.

The longitudinal distribution of the low-latitude radial currents is presented in Figure 5. In Figure 5 (top) we show the current intensity from the time sector around noon. As expected we find upward currents in the Southern Hemisphere. However, the downward currents in the Northern Hemisphere are interrupted by a weak but significant upward current in the latitude range 5°–10° MLAT and around the 300°E GLon sector. This current feature reduces the IHFAC intensity and is probably the reason for the minimum in noontime IHFAC evident in Figure 3. The downward *F* region dynamo current is stronger in the longitude sector 0°E–210°E than in the other part.

Figure 5 (bottom) shows the latitude versus longitude distribution from the evening sector. At that time all low-latitude current is flowing upward. Due to the small current density scale range the plot appears rather scattered. For the *F* region dynamo current, only the ±5° MLAT range is of interest. We can see that the dynamo currents at evening are strongest in the longitude range 150°E–300°E GLon. In the next section we try to provide explanations for the observation.

5. Discussion

Initial results about *F* region currents derived with the Swarm constellation over the period 17 April to 5 November 2014 have been presented. It became evident that interhemispheric field-aligned and *F* region dynamo currents have to be interpreted simultaneously in order to fully understand the observations.

IHFACs are about 4 times stronger than the *F* region dynamo currents. Therefore, it makes sense to interpret them first. In general, our observations confirm the theoretical expectation of a major current flow from winter to the summer hemisphere. For detailed inspections our Figure 3 can be compared with Figures 5 (top) and 6 (top) in *Park et al.* [2011]. These authors found that IHFAC characteristics are much the same during the months May through September. However, they have used another convention for current direction, negative values represent currents from south to north. In general, the results of both studies agree well. We obtain around noon mean current densities of about 13 nA/m^2. When assuming that these flow over a latitude range of 2000 km, we obtain a sheet current density of 26 mA/m. This is somewhat higher than the value (about 20 mA/m) reported by *Park et al.* [2011]. It is interesting to note that the weak IHFAC around 330°E GLon is related by *Park et al.* [2011] to the South Atlantic Anomaly. Also, the shift of the current peak to earlier local times in the sector 200°E–300°E GLon can be found in their study. Both these features are more prominent in *Park et al*. [2011] probably due to their much longer data interval.

Quite unexpected is the appearance of an upward current in the northern low-latitude hemisphere around the 270°E–330°E longitude range (see Figure 5, top). Corresponding to that we find a significant weakening of the upward current in the Southern Hemisphere. Our preferred interpretation is that these current features are related to the South Atlantic anomaly (SAA). In this region of the weak geomagnetic field the *Sq* current system is expected to be enhanced. Studies of *Takeda* [1996] suggested that a weak *B* field shifts the dynamo altitude upward where the plasma density and wind speed are higher. As a consequence of that summer-like *Sq* conditions are expected in the SAA region even during local winter. Thus, in this longitude sector the potential difference to the Northern Hemisphere is reduced or even reversed locally.

Our observations provide also a detailed picture of the *F* region dynamo currents. A schematic illustration of the complete current system, including vertical currents above the dip equator and meridional currents connecting them to the *E* regions in the two hemispheres, is given in *Lühr and Maus* [2006, Figure 2]. As expected, we find downward currents around noon and upward around sunset. The typical current density of 3 nA/m^2 is quite low but well recovered with Swarm. The vertical current sheet is rather narrow, only ±2.5° in latitude around noon and about twice of that in the evening sector. This means that the dynamo is efficient only in the close vicinity of horizontal magnetic field lines. Any deviation from that is obviously shorted out by FACs connecting to the *E* region. Along this line of argument we may also explain the somewhat wider vertical current sheet in the evening, when the *E* layer conductivity is reduced. When assuming a triangular

©2015. American Geophysical Union. All Rights Reserved.

latitude profile of current density we obtain sheet current densities of about 1 mA/m for both time sectors. This can be compared with the values reported by *Park et al.* [2010a]. When considering the mean solar flux of our data period, $F_{10.7} = 140$ solar flux unit, we read from their Figure 6 annual averages of 2 mA/m and 1.3 mA/m for the noon and evening time sectors, respectively. Our lower numbers can be explained by the fact that we have sampled mainly June solstice conditions when *F* region dynamo currents are weakest [see *Park et al.*, 2010a, Figure 3].

From Figure 5 it is obvious that the noontime dynamo currents are stronger at longitudes 0°E–210°E. This is the longitude range where the dip equator is located in the Northern Hemisphere. Here we can expect enhanced conductivity due to summer conditions. In the evening radial currents are strongest in the sector 150°E–300°E GLon. This is the range over which the dip equator changes from the Northern to the Southern Hemisphere. Here the magnetic field and L shells are declined toward east. Thus, the footprints in the *E* layer of the *F* region dynamo are well aligned to the summertime evening terminator. This causes a stronger zonal gradient of the flux tube-integrated conductivity. It has been shown by *Park et al.* [2010b] that the strength of *F* region currents is proportional to the zonal gradient of the flux tube conductance.

From Figure 5 it is obvious that the noontime dynamo currents are stronger at longitudes 150°E–330°E, and the evening currents are weakest in that sector. Zonal winds from CHAMP provide no suitable explanation for that longitudinal variation. *Park and Lühr* [2013] showed that *E* region dynamics has a strong influence on the *F* region currents. We may well see the response of a tidal effect at *E* layer altitude.

6. Summary

F region currents at low latitudes have for the first time been deduced from dual-satellite observation using the Swarm constellation. Here we present initial results from the first half year of formation flight. Our data confirm, in general, for the interhemispheric field-aligned currents (IHFAC) and the *F* region dynamo currents the expected and previously reported characteristics during June solstice and September equinox seasons. The new approach, however, provides more significant results and more details. Important findings are the following:

1. Sizable field-aligned currents, but about 100 times smaller than auroral FACs, are flowing from the Southern (winter) Hemisphere into the Northern around noontime. Weaker currents with directions opposite to noon are observed during morning and evening hours. This is largely consistent with the predicted picture for June solstice, except for the current direction during evening hours.
2. IHFACs in all three local time sectors show intensity variations with longitude. Quite prominent is the weakening of the noontime IHFAC around 330°E GLon. We suggest also a relation to the South Atlantic anomaly. In the low magnetic field region *Sq* currents are expected to be stronger. Thus, the potential difference to the Northern Hemisphere at summer conditions is reduced.
3. Right above the dip equator weak vertical *F* region dynamo currents are flowing, downward around noon, and upward at about 18 MLT. These currents are confined to a narrow latitude range, ±2.5° around noon and ±5° at 18 MLT.
4. The dynamo current intensity also exhibits longitudinal variations. During noontime the vertical currents are enhanced over the longitude range 0°E–210°E, where the dip equator lies in the Northern (summer) Hemisphere. Radial currents in the evening sector are strongest over the longitude range 150°E–300°E. Here the eastward declined flux tubes are well aligned with the summertime evening terminator. This results in a strong zonal gradient of the flux tube-integrated conductivity.

These initial data from dual-satellite analysis have provided promising results. Longer series of data over years, however, are needed to determine special features of these *F* region currents including seasonal and solar flux dependences, their modulation by atmospheric tides and meteorological phenomena.

Acknowledgments
The European Space Agency (ESA) is acknowledged for providing the Swarm data and for financially supporting the work described in this paper. The data used here are the Swarm Level-1b MAGNET data freely accessible at https://earth.esa.int/web/guest/swarm/data-access. In case of interest in higher-level products, please contact the corresponding author.

The Editor thanks Joseph Huba and W. Jeffrey Hughes for their assistance in evaluating this paper.

References

Campbell, W. H. (1989), The regular geomagnetic field variations during quiet solar conditions, in *Geomagnetism*, vol. 3, edited by J. A. Jacobs, pp. 385–460.

Friis-Christensen, E., H. Lühr, D. Knudsen, and R. Haagmans (2008), Swarm—An Earth observation mission investigating Geospace, *Adv. Space Res.*, *41*, 210–216, doi:10.1016/j.asr.2006.10.008.

©2015. American Geophysical Union. All Rights Reserved.

Fukushima, N. (1979), Electric potential difference between conjugate points in middle latitudes caused by asymmetric dynamo in the ionosphere, *J. Geomagn. Geoelectr.*, *31*, 401–409.

Fukushima, N. (1994), Some topics and historical episodes in geomagnetism and aeronomy, *J. Geophys. Res.*, *99*(A10), 19,113–19,142, doi:10.1029/94JA00102.

Liu, H., H. Lühr, S. Watanabe, W. Köhler, V. Henize, and P. Visser (2006), Zonal winds in the equatorial upper thermosphere: Decomposing the solar flux, geomagnetic activity, and seasonal dependencies, *J. Geophys. Res.*, *111*, A07307, doi:10.1029/2005JA011415.

Lühr, H., and S. Maus (2006), Direct observation of the *F* region dynamo currents and the spatial structure of the EEJ by CHAMP, *Geophys. Res. Lett.*, *33*, L24102, doi:10.1029/2006GL028374.

Maeda, H., T. Iyemori, T. Araki, and T. Kamei (1982), New evidence of a meridional current system in the equatorial ionosphere, *Geophys. Res. Lett.*, *9*(4), 337–340.

Matsushita, S., and H. Maeda (1965), On the geomagnetic solar quiet daily variation field during the IGY, *J. Geophys. Res.*, *70*(11), 2535–2558, doi:10.1029/JZ070i011p02535.

Olsen, N. (1997), Ionospheric *F* region currents at middle and low latitudes estimated from Magsat data, *J. Geophys. Res.*, *102*(A3), 4563–4576, doi:10.1029/96JA02949.

Park, J., and H. Lühr (2013), Relation of zonal plasma drift and wind in the equatorial *F* region as derived from CHAMP observations, *Ann. Geophys.*, *31*, 1035–1044, doi:10.5194/angeo-31-1035-2013.

Park, J., H. Lühr, and K. W. Min (2010a), Characteristics of *F*-region dynamo currents deduced from CHAMP magnetic field measurements, *J. Geophys. Res.*, *115*, A10302, doi:10.1029/2010JA015604.

Park, J., H. Lühr, B. G. Fejer, and K. W. Min (2010b), Duskside *F*-region dynamo currents: Its relationship with prereversal enhancement of vertical plasma drift, *Ann. Geophys.*, *28*, 2097–2101.

Park, J., H. Lühr, and K. W. Min (2011), Climatology of the inter-hemispheric field-aligned current system in the equatorial ionosphere as observed by CHAMP, *Ann. Geophys.*, *29*, 573–582, doi:10.5194/angeo-29-573-2011.

Rishbeth, H. (1971), The F-layer dynamo, *Planet. Space Sci.*, *19*, 263.

Ritter, P., H. Lühr, and J. Rauberg (2013), Determining field-aligned currents with the Swarm constellation mission, *Earth Planets Space*, *65*, 1285–1294, doi:10.5047/eps.2013.09.006.

Takeda, M. (1996), Effects of the strength of the geomagnetic main field strength on the dynamo action in the ionosphere, *J. Geophys. Res.*, *101*(A4), 7875–7880.

van Sabben, D. (1964), North-south asymmetry of S_q, *J. Atmos. Terr. Phys.*, *26*, 1187–1195.

Yamashita, S., and T. Iyemori (2002), Seasonal and local time dependences of the interhemispheric field-aligned currents deduced from the Ørsted satellite and the ground geomagnetic observations, *J. Geophys. Res.*, *107*(A11), 1372, doi:10.1029/2002JA009414.

Yamazaki, Y., et al. (2011), An empirical model of the quiet daily geomagnetic field variation, *J. Geophys. Res.*, *116*, A10312, doi:10.1029/2011JA016487.

 ©2015. American Geophysical Union. All Rights Reserved.